A STATISTICAL ANALYSIS OF INDOOR MULTIPATH FADING FOR A NARROWBAND WIRELESS BODY AREA NETWORK

Simon L. Cotton
Institute of Electronics, Communications & IT
The Queen's University of Belfast,
Belfast, BT3 9DT,UK
s.cotton@ieee.org

William G. Scanlon
Institute of Electronics, Communications & IT
The Queen's University of Belfast,
Belfast, BT3 9DT,UK
w.scanlon@qub.ac.uk

ABSTRACT

A thorough statistical analysis of multipath effects for on-body propagation channels in wireless body area networks (WBANs) is presented. Experiments were conducted at 868 MHz for both stationary and mobile scenarios in an anechoic chamber and two typical indoor environments. When the WBAN is stationary, fading in bodyworn channels is determined by body-centric processes with Nakagami fading ($m >> 1$) shown to provide the optimum fit. Equivalent Rician K_{dB}-factors for these channels are also shown to be high, peaking at 36.1 dB for channels which cross the anterior chest region. However, mobile fading channels were predominantly Rice distributed in multipath environments. Movement in a multipath environment also caused a reduction in m and K values beyond that observed in anechoic conditions.

I. INTRODUCTION

WBAN designers are presented with a number of significant challenges not seen in the implementation of traditional personal area networks (PAN). WBAN nodes are expected to have a low profile form factor, operate efficiently and be non-interfering with movement. Proposed WBAN applications include medical sensor networks used for tether-less patient monitoring. These applications usually require low data rates so protocols based on the IEEE 802.15.4 standard such as ZigBee [1] are used. Therefore, in this work we focussed on the European Industrial, Scientific and Medical band at 868 MHz.

The radiowave propagation mechanisms which define the bodyworn channel are extremely complex due to the distinctive multipath and scattering effects encountered. In anechoic conditions a link between two points on the body may be formed by radio waves passing through tissue or travelling around the body surface [2] if there is no direct line of sight (LOS) path available. Antennas designed for bodyworn applications tend to be restricted in dimensions and therefore electrically small meaning that close proximity effects [3, 4] caused by antenna-body coupling are much more significant. Time-varying shifts in antenna position and orientation caused by movement and respiration can cause radiation pattern fragmentation and alternating antenna impedance leading to an overall reduction in system efficiency. In an indoor environment the perturbation in received signal may be further exacerbated by strong reflections from nearby objects inclusive of persons and building structures [5].

On-body propagation channels have been studied in [6,7] but most of the published work to-date is restricted to experimental investigations utilising coaxial cables, antennas and a vector network analyzer to measure forward gain. In this work a distributed narrowband measurement system, capable of synchronously monitoring received signal strength indication (RSSI) at sub 4 ms intervals for individual on-body channels, was used. A network of individual radio frequency (RF) transceivers was used to investigate both stationary and mobile user scenarios at 868 MHz within three different indoor environments. Twelve on-body propagation paths, spanning the upper torso and limbs, were considered. The results were analysed using maximum likelihood estimation (MLE) and the Akaike information criterion (*AIC*) [8], for parameter and model selection, respectively.

II. MEASUREMENT SYSTEM, ENVIRONMENT AND PROCEDURE

A. System

The bodyworn measurement system consisted of six self-contained data logging Crossbow Mica2Dot wireless sensor motes and a NovaSource G6 signal source that was configured to deliver –13 dBm of continuous wave through a vertically polarized λ/4 stub antenna. Each of the RSSI sensing motes was individually pre-calibrated and had a modified 3.6 V, 0.95 Ah lithium-thionyl chloride power supply unit and a helical antenna mounted on a 25.4 mm circular ground plane (Fig. 1). A 10-bit on-board analogue to digital converter was used to quantize the RSSI voltage from the mote's Chipcon CC1000 RF chip. The mote software allowed sharing of the timing information so that all measurements were synchronous.

Fig. 1. Measurement system.

1-4244-0330-8/06/$20.00©2006 IEEE

The RF source was mounted at the test person's waist or chest and, to minimize spurious antenna-body separation effects, each of the motes fixed to a 3 mm thick, tight fitting, polychloroprene / nylon contoured jacket. The six receiver locations were: lower left abdomen, left chest, left wrist, right wrist, back left and back right (from the test subject's perspective), giving a total of twelve on-body propagation channels.

B. Environment

Measurements were taken in three separate environments: anechoic chamber, open office area and hallway all situated on the ground floor of the ECIT building at Queen's University Belfast, UK (Fig. 2). The building was of recent construction. The open office area (244.2 m^2) and hallway (13.5 m^2) consisted mainly of metal studded dry wall with a metal tiled floor covered with polypropylene-fibre, rubber backed carpet tiles, and a metal ceiling with mineral fibre tiles and recessed louvered luminaries suspended 2.7 m above the floor level. The open office area also contained a number of soft partitions, PCs, chairs and desks constructed from medium density fibreboard. The 54 m^2 anechoic chamber was lined with pyramidal RF absorbers.

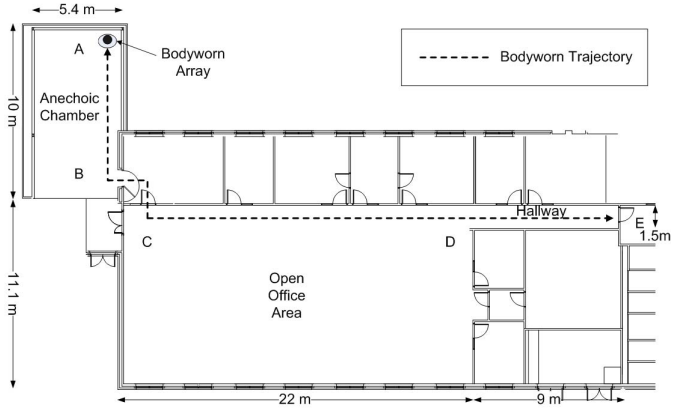

Fig. 2. Plan view of measurement location.

C. Procedure

RSSI voltage was measured in a continuous recording session which meant that cross-body channels for each scenario could be directly compared. The test user was an adult male of mass 83 kg and height 1.72 m. The user was instructed to stand motionless at the starting position in the anechoic chamber (point A in Fig. 2) with the RF source at his waist. All units were then activated to make synchronous measurements of the RSSI voltage at 3.91 ms intervals. After 20 s the transmitter was momentarily keyed off to allow a recognizable break in the results. The test subject then began to walk in a natural manner along the trajectory shown to point B. This process was repeated via points C, D and E where further static user measurements were made. Upon completing the stationary observations at E, the transmitter was transferred to the test person's chest and the reverse journey completed. Stationary measurements made at E were used in the analysis of the hallway environment presented in section IV.

III. Channel Characterisation

A. Nakagami, Rician and Rayleigh Fading

The probability density function (pdf) of the Nakagami-*m* distribution for the normalised signal of amplitude *r* is given by:

$$p(r \mid m,\Omega) = \frac{2}{\Gamma(m)}\left(\frac{m}{\Omega}\right)^{m} r^{2m-1}\exp\left\{-\left(\frac{mr^2}{\Omega}\right)\right\} \quad (m \geq \frac{1}{2}, r \geq 0) \quad (1)$$

where Ω is the mean square, *m* is the fading parameter and $\Gamma(\cdot)$ is Euler's Gamma function.The Nakagami-*m* distribution describes in an approximate way the distribution of a vector process where the central limit theorem is not necessarily valid [9]. The Rice distribution represents the superposition of a deterministic dominant component (*A*) on a zero mean, Gaussian distributed diffuse signal contribution σ. The Rice pdf may be represented by:

$$p(r \mid A,\sigma) = \frac{r}{\sigma^2}\exp\left\{-\left(\frac{r^2+A^2}{2\sigma^2}\right)\right\} I_0\left(\frac{Ar}{\sigma^2}\right) \quad (A \geq 0, r \geq 0) \quad (2)$$

$I_0(\cdot)$ is a modified Bessel function of the first kind and zero order. The Rican-*K* factor is often used to describe the Rice distribution and is defined as the ratio of the square of the dominant component over the (local mean) scattered power. In equation (1), when $m > 1$, the Nakagami-*m* distribution may be used to approximate the Rice distribution. This leads to the following approximation of the Rician-*K* factor using the Nakagami-*m* parameter [9]:

$$K = \frac{\sqrt{m^2 - m}}{m - \sqrt{m^2 - m}}. \quad (3)$$

In the absence of a dominant component ($A = 0$) the Rician pdf degenerates into a Rayleigh distribution:

$$p(r \mid \sigma) = \frac{r}{\sigma^2}\exp\left\{-\left(\frac{r^2}{2\sigma^2}\right)\right\}. \quad (4)$$

The Nakagami-*m* distribution (1) also has a Rayleigh equivalent which occurs when $m = 1$.

B. MLE of Distribution Parameters

For the Rayleigh distribution given in (4), if $r_1, r_2, \ldots r_n$ are independent observations of the received signal then the joint probability of the observations is

$$L(\sigma \mid R) \equiv p(R \mid \sigma) = \prod_{i=1}^{n} p(r_i \mid \sigma). \quad (5)$$

$L(\cdot)$ represents the likelihood function which is the probability of obtaining σ given the received envelope *R*. The *posteriori* probability of a Rayleigh distributed envelope may be expressed in the form:

$$L(\sigma \mid R) = \prod_{i=1}^{n} (r_i)(\sigma^{-2n})\exp\left\{-\sum_{i=1}^{n}\left(\frac{r_i^2}{2\sigma}\right)\right\}. \quad (6)$$

The parameter σ for which the likelihood function is a maximum is found by first taking the logarithm of (6)

$$\log(L(\sigma \mid R)) = \sum_{i=1}^{n}\log(r_i) - 2n\log(\sigma) - \sum_{i=1}^{n}\left(\frac{r_i^2}{2\sigma}\right). \quad (7)$$

Now differentiation is made easier as the repeated multiplication has been converted to addition. To obtain a maximum (assuming the likelihood is unimodal) the partial differential of (7) is taken with respect to σ and the result set to equal 0. With some rearrangement the efficient estimator of σ is given by:

$$\hat{\sigma} = \sqrt{\sum_{i=1}^{n}\left(\frac{r_i^2}{2n}\right)}. \quad (8)$$

The log-likelihood reaches a maximum at the same point as the original function and the nature of the stationary point may be determined from its second derivative. As σ is a single parameter the Hessian (matrix of partial second derivatives) is scalar. The Fisher information ($I(\sigma)$) is now

$$I(\sigma) = -E\left[\frac{2n}{\sigma^2} - \sum_{i=1}^{n}\left(\frac{r_i^2}{3\sigma^4}\right)\right]. \quad (9)$$

$E[.]$ is the mathematical expectation. Taking the square root of $I(\sigma)^{-1}$ yields the estimated standard error. The interested reader is directed to Nakagami-*m* [10] and Rice [11] for maximum likelihood parameter estimation of these distributions.

C. Model Selection

Model selection in this paper uses the sum of the squared errors (*SSE*) in conjunction with the entropy based *AIC*. The *SSE* between the empirical cumulative distribution $g(r_i)$ and the MLE predicted distribution $\hat{g}(r_i)$ is

$$SSE = \sum_{i=1}^{n}\left(g(r_i) - \hat{g}(r_i)\right)^2. \quad (9)$$

When using *SSE*, Burnham and Anderson [13] suggest the following analogue of the *AIC:*

$$AIC = n\log\left(\frac{SSE}{n}\right) + 2P, \quad (10)$$

where n is the number of data points and P is the number of estimated parameters. The *AIC* stipulates that the model with the lowest *AIC* score provides the best fit.

VI. RESULTS

A total of 31,340 samples of received power were logged at a rate of 256 Hz. The data was analysed for 12 distinct on-body transmission paths in the three different environments. The results for each environment are subdivided into two categories, stationary and mobile, resulting in 72 scenarios. Average straight line velocity was estimated from the results as 2 ms^{-1} using the time taken to traverse the distance between the two points C and D in Fig. 2. Assuming that the body is the predominant scattering object in each environment, the mobile results were subject to a scatterer shift of approximately $\lambda/44$, where $\lambda = 0.345$ m. For all mobile measurements, the local mean was calculated by averaging over 1λ. For user static measurements the mean values were simply the average of the received envelope for that session. Noise floor measurements were made for each of the bodyworn devices immediately prior to the experiment in each location and are shown in Table 1.

Table 1: Noise floor measurements for each of environment.

Environment	Noise Floor Mean (dBm)	Noise Floor Std. Dev. (dB)	Lowest Recorded Sample (dBm)
Anechoic Chamber	–97.0	2.7	–86.8
Open Office Area	–96.5	2.6	–90.2
Hallway	–96.4	2.7	–85.8

A. Anechoic chamber

When stationary in the chamber, the mean received signal was higher for propagation paths that crossed the front of the upper torso. The difference between the right chest to left chest, which experienced the highest mean RSSI, and right waist to back right, the poorest performing link, was approximately 30 dB (Fig. 3). Fast fading due to breathing and other body movements ranged between 0.6 dB (right chest to right wrist) and 3.0 dB (right waist to back right). The latter is similar to published results [6] for a waist to shoulder link at 2.45 GHz.

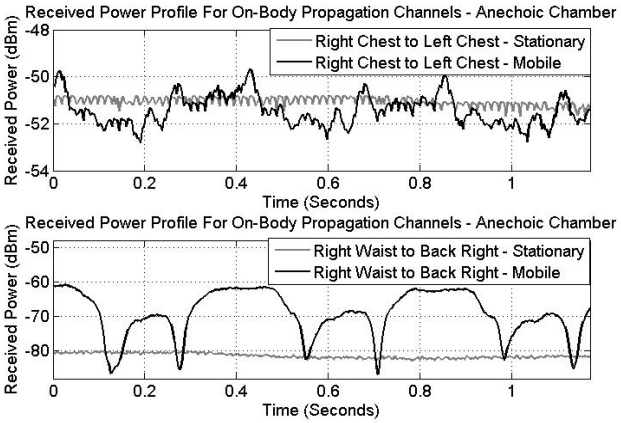

Fig. 3. Received power profiles (RPPs) for example on-body propagation channels in the anechoic chamber.

Table 2 presents MLE distribution parameters and *AIC* indexes for a selection of the bodyworn channels fitted to Nakagami-*m*, Rice and Rayleigh cumulative density functions (CDFs). All parameters were calculated on a 95% confidence interval (CI). Table 2 also shows quite clearly the robustness of the Nakagami-*m* parameter as an estimator of the Rician-*K* factor. Based on *AIC* scoring the Nakagami distribution out performed the Rician and Rayleigh distributions in 11 out of the 12 stationary in-chamber measurements. Nakagami-*m* figures for these channels were >> 1. As $m \to \infty$, the Nakagami pdf approaches a delta function (no fading). Therefore respiratory related effects such as displacement of antennas, varying antenna-body coupling and variations in body shape caused only minor changes in the channel. This is supported by the Rician-*K* factors (in dB) for these channels (calculated using the fitted Rician distributions) which were extremely high, with a mean of 26.9 dB and a standard deviation of 2.8 dB. The Nakagami-*m* distribution can also work under conditions where the possibility of partial

correlation exists between scattering elements [12]. This is in contrast to the Rice and Rayleigh pdfs which require random scattered components. Since it is a reasonable expectation that fading and body centric processes are partially correlated, it is not surprising that Nakagami-*m* provides the optimum fit for on-body channels in the anechoic chamber.

When the user was in motion all paths, with the exception of the right waist to right wrist, showed an increase in mean signal level. Greatest signal variation (25.8 dB) was observed in the right waist to back right path (Fig. 3). This was surprising as it was expected that paths incorporating the wrists would experience the largest change in received signal as the transmitter-receiver separation would be periodically changing, with link conditions alternating between LOS and non line of sight (NLOS). Figure 4 shows the CDF for the right chest to back right on-body propagation channel. In the anechoic chamber, four of the mobile channels were best characterised by a Rician distribution, the remaining eight were Nakagami distributed. Both the Nakagami-*m* (mean = 58.32) and the fitted Rician-K_{dB} (mean = 19.7 dB) factors remained high although spread increased mainly due to lower *K* values for the channels which showed Rician predominance (standard deviation, 8.4 dB). Changing posture caused by movement may have added to the scattered wave contribution through increased partial body reflections. The resultant superimposed on the dominant cross-body path will cause a reduction in both *m* and *K* values.

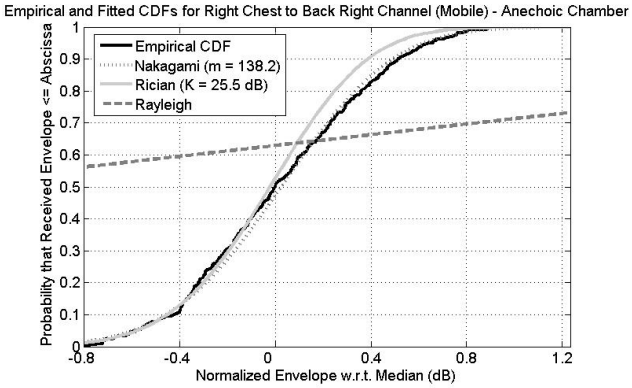

Fig. 4. Empirical and MLE Fitted CDF for right chest to back right transmission mobile path in the anechoic chamber.

B. Open Office Area

Under the multipath conditions of the open office area, the average signal levels when stationary were within ±3 dB of those in the chamber. The only exception was the right waist to back right path in which the mean power level rose by 13 dB. A possible explanation for this difference was the fact that the back right receiver had been positioned in a fade for the duration of the measurements in the chamber. Ryckaert *et al* [2] discuss the interaction of surface waves which choose different directions around the body. A creeping wave that turns clockwise may interfere with one that travels anticlockwise. However, another study, currently in press, by the authors shows that receivers on the upper torso are highly unlikely to remain in a fade for any significant length of time due to respiration effects. Nonetheless, the optimal fading model selection for the stationary open office CDFs were largely identical to those for the anechoic chamber. Eleven out of the twelve paths were Nakagami distributed. Equivalent Rician K_{dB}-factors remained high with an average of 26.2 dB and standard deviation 4.0 dB. From this it may be deduced that on-body propagation, when the user is stationary, is governed largely by processes which are local to the body with environmental factors playing a reduced role in channel statistics.

Fig. 5 shows an alternating pattern of signal maxima and minima for the right waist to right wrist path as the user moved through the open office. This is caused by shadowing as the wrist worn node oscillates between LOS and NLOS experiencing fades of up to 10 dB from the local mean. This was indicative of profiles for paths in which both transmitter and receiver were located on parts of the body which were in motion relative to one another. The typical dynamic range for fading was approximately 18 dB for the right waist to right wrist link and 30 dB for the right waist to a back mounted receiver.

Table 2: MLE parameter estimated and *AIC* scores for a selection of transmission paths (stat = stationary, est = estimate).

Transmission Path	Environment	State	Distribution	*AIC*	Parameter Estimate	Mean (dBm)	Std. Dev. (dB)	Range (dB)	Rician-*K* (dB)
Right Chest to Back Left	Anechoic Chamber	stat	Nakagami-*m*	–154.0	$m = 146.95$ $\Omega = 0.99$	–77.3	0.4	2.0	24.7(est)
			Rice	–121.6	$A = 1.00$ $\sigma = 0.04$				25.0
			Rayleigh	–48.4	$\sigma = 0.70$				
Right Chest to Back Left	Anechoic Chamber	mobile	Nakagami-*m*	–1206.8	$m = 4.99$ $\Omega = 1.03$	–76.0	2.4	12.9	9.3 (est)
			Rice	–1263.2	$A = 0.96$ $\sigma = 0.22$				9.6
			Rayleigh	–599.5	$\sigma = 0.72$				
Right Chest to Back Left	Open Office Area	mobile	Nakagami-*m*	–1269.3	$m = 1.44$ $\Omega = 1.20$	–71.6	5.0	28.6	0.9 (est)
			Rice	–1567.0	$A = 0.88$ $\sigma = 0.46$				2.6
			Rayleigh	–965.6	$\sigma = 0.77$				

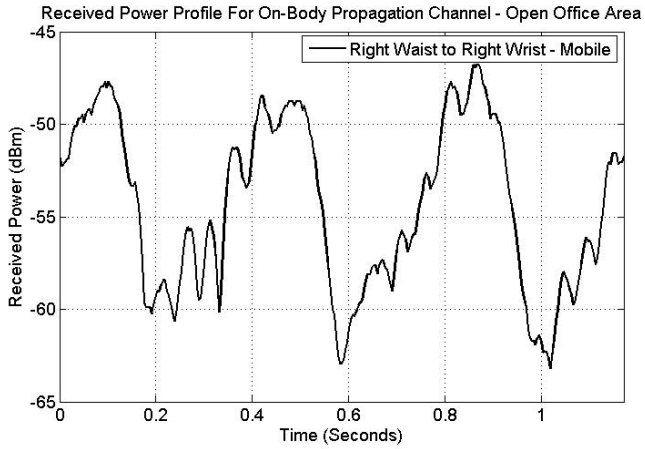

Fig. 5. RPP for the right waist to right wrist mobile on-body path in the open office area.

The *AIC* scores calculated for the mobile results in the open office area showed that a Rician CDF described fading for 7 of the 12 paths. Increased field perturbation generated by limb movement and reflections from nearby surfaces caused a reduction in *m* and *K* values beyond those observed in the chamber (Fig. 4 and 6). Mobile power levels in the open office were mostly within 1 dB of those observed in the chamber. However, the dynamic range increased for all paths suggesting that multipath effects are an important consideration.

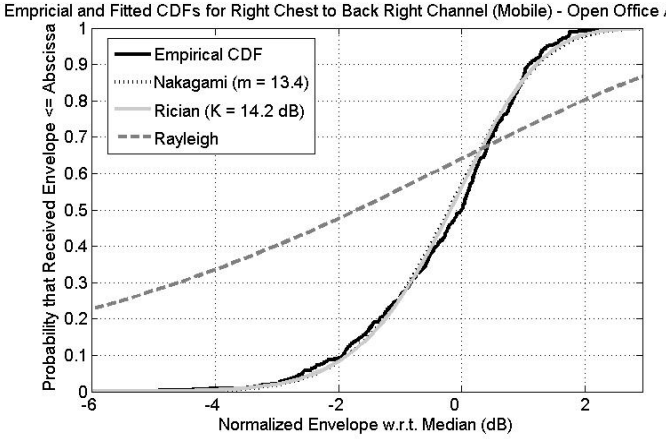

Fig. 6. Empirical and MLE Fitted CDF for right chest to back right transmission path moving in open office area.

C. Hallway

Measurements taken in the hallway environment were similar to those for the open office area in both stationary and mobile cases. Nakagami distributions described stationary on-body paths and Rician fading dominated the mobile ones. Compared to the open office area, Nakagami-*m* and Rician-*K* factors were similar when stationary and on average, K_{dB} was 1.5 dB greater when mobile. This was unexpected due to the decreased distance between the bodyworn devices and upright structures which may have increased the scattered power component.

V. CONCLUSIONS

The statistical analysis of fading environments on narrowband on-body propagation paths has identified a number of different important characteristics. Overall, over two thirds of the paths investigated were Nakagami distributed with the remainder Rician. The majority of the Nakagami paths were observed when the user was stationary. Increased field perturbation caused by movement added to the random diffuse component, resulting in lower Nakagami-*m* values and *AIC* scores that favour Rician fading models. All Nakagami distributed channels provided Rician equivalents with high *K*-factors.

These results also suggest that special consideration should be given to the placement of WBAN nodes on the posterior shoulder region especially when the opposite end of the link is located on the anterior waist region. These channels are susceptible to up to 30 dB dynamic range when the user is in motion. Maximum signal attenuation is also experienced here. In terms of mean RSSI, high K_{dB}-factors (>35 dB) and reduced fading (typically less than 1 dB), the best paths occur for user-stationary channels which cross the upper front chest area. These channels also show resilience to the effects of time variant fading with a dynamic range less than 6 dB. Finally, on-body paths which utilise free space propagation such as nodes situated on the wrists will be subject to cyclic variations in received signal when the user is mobile.

REFERENCES

[1] ZigBee Alliance, "ZigBee Document 053474r06, Version 1.0," vol. 1, June. 2005.

[2] J. Ryckaert, P. Doncker, R. Meys, A. de Le Hoye and S. Donnay, "Channel model for wireless communication around human body," *Electronic Letters*, vol. 40, April. 2004.

[3] H.R. Chuang, "Human operator coupling effects on radiation characteristics of a portable communication dipole antenna," *IEEE Trans. on Antennas and Prop.*, vol. 42, pp. 556-560, April. 1994.

[4] W. Scanlon and N. Evans, "Numerical analysis of bodyworn UHF antenna systems," *Electronics and Communications. Journal*, pp. 53-64, April. 2001.

[5] R. Bultitude, "Measurement, characterization and modelling of indoor 800/900 MHz radio channels for digital communications," *IEEE Communications Magazine*, vol. 25, pp. 5-12, June. 1987.

[6] P. Hall, M. Ricci and T. Hee, "Measurements of on-body propagation characteristics," *IEEE Antennas and Prop. Soc. Int. Symp.*, 2002, pp. 310-313.

[7] A. Alomainy, Y. Hao, C. Parini and P. Hall, "Comparison between two different antennas for UWB on-body propagation measurements," *IEEE Antennas and Wireless Prop. Letters*, vol. 4, pp. 31-34, 2005.

[8] H. Akaike, "A new look at the statistical model identification," *IEEE Trans. on Automatic Control*, vol. 19, pp. 716-723, 1974.

[9] A. Molisch, *Wireless communications*, IEEE Press, Wiley, 2005.

[10] J. Cheng and N. Beaulieu, "Maximum-likelihood based estimation of the Nakagami m parameter," *IEEE Comms. Letters*, vol. 5, pp. 101-103, 2001.

[11] J. Sijbers, A.J. den Dekker, P. Scheunders and D. Van Dyck, "Maximum-likelihood estimation of Rician distribution parameters," *IEEE Trans. on Medical Imaging*, vol. 17, pp. 357-361, 1998.

[12] P. Shankar, *Introduction to wireless systems*, Wiley, 2001.

[13] K.P. Burnham and D.R. Anderson, "Multimodel Inference: understanding AIC and BIC in Model Selection," *Amsterdam Workshop on Model Selection*, 2004, pp. 1-56.